

**Supporting Information for**  
**Manifesting the Sergeants-and-Soldiers Principle in**  
**Coadsorber Induced Homochiral Polymorphic Assemblies**  
**at the Liquid/Solid Interface**

Shu-Ying Li,<sup>a,b</sup> Ting Chen,<sup>a</sup> Jie-Yu Yue,<sup>a,b</sup> Lin Wang,<sup>a,b</sup> Hui-Juan Yan,<sup>a</sup> Dong Wang,<sup>\*a</sup> and Li-Jun  
Wan<sup>\*a</sup>

<sup>a</sup> Key Laboratory of Molecular Nanostructure and Nanotechnology and Beijing National  
Laboratory for Molecular Sciences, Institute of Chemistry, Chinese Academy of Sciences (CAS),  
Beijing 100190, P.R. China

<sup>b</sup> University of Chinese Academy of Sciences, Beijing 100049, P.R.China.

**Contents:**

1. Experimental materials and methods
2. STM images of the BIC-C6 and BIC-C8 honeycomb networks
3. STM images of the BIC monolayers in the presence of (*R*)-2-nonanol and (*S*)-2-nonanol
4. The energy gain when an co-adsorbed 1-octanol in CW domain is replaced by (*R*)-2-nonanol
5. MM simulations using Dreiding force field
6. Another unfavorable conformation

## 1. Experimental materials and methods

**Experimental details.** BIC derivatives were synthesized as described in a previous report<sup>1</sup>. Concentration of BIC in solutions used in the present study is all the same ( $2 \times 10^{-4}$  M). Chiral 2-nonanol was used as solvent in this study and purchased from sigma-aldrich with purity of 99%. To form a BIC assembly, a droplet of BIC solution was dropped onto a freshly cleaved HOPG (grade ZYB) surface. STM tips were mechanically cut from Pt/Ir wire (90/10). STM experiments were performed using PicoSPM (Agilent Technologies) in constant-current mode at room temperature. All STM images were shown without any modification.

**Statistical methods.** Distributions of the enantiomorphs on surface for each sample were recorded based on more than 60 large-scale STM images ( $100 \times 100$  nm<sup>2</sup>) obtained at different locations. Note that the organizational chirality given in this paper is an average value of several investigated samples.

**Molecular mechanistic simulations.** MM simulations were carried out with the molecular package TINKER using the MMFF force field<sup>2-4</sup>. 2D packing models of BIC were built according to the STM images. The BIC monolayers are placed 0.35 nm above the upper layer of a two-layer sheet of graphite keeping the alkyl chains in BIC parallel to the directions of graphite symmetry axes. During optimization, the graphite was frozen. As processed in previous literature<sup>5</sup>, the calculated results from MM simulations are divided by the area possessed by the hexagonal network. Thus, the energy data provided in the text indicate the packing energy density in different networks.

## 2. STM images of the BIC-C6 and BIC-C8 honeycomb networks.

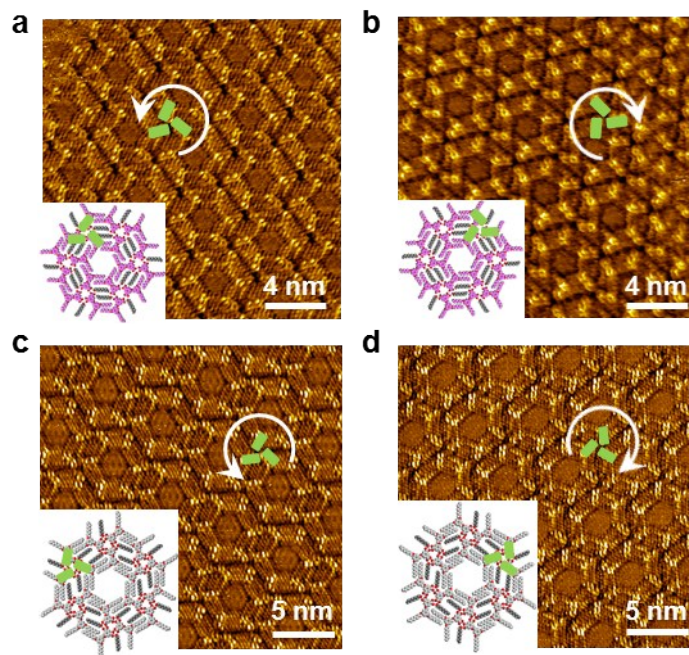


**Figure S1. STM images of the BIC monolayers at the 1-octanol/HOPG interface.** (a) Counterclockwise (CCW) domains in BIC-C6 assembly; (b) Clockwise (CW) domains in BIC-C6 assembly; (c) CCW domains in BIC-C8 assembly; (d) CW domains in BIC-C8 assembly. Tunneling parameters: average tunneling current ( $I_{\text{set}}$ ) = 0.5–1 nA, bias voltage ( $V_{\text{bias}}$ ) = 900 mV. Green sticks outline the bright aromatic cores in BIC and are combined to indicate a BIC trimer in the assembly. White arrows identify the handedness of the trimer. Insets depict the molecular models in corresponding monolayer. BIC-C6 and BIC-C8 are colored pink and light gray for identification. 1-octanol is colored dark grey for clarity.

### 3. STM images of the BIC monolayers in the presence of (*R*)-2-nonanol and (*S*)-2-nonanol

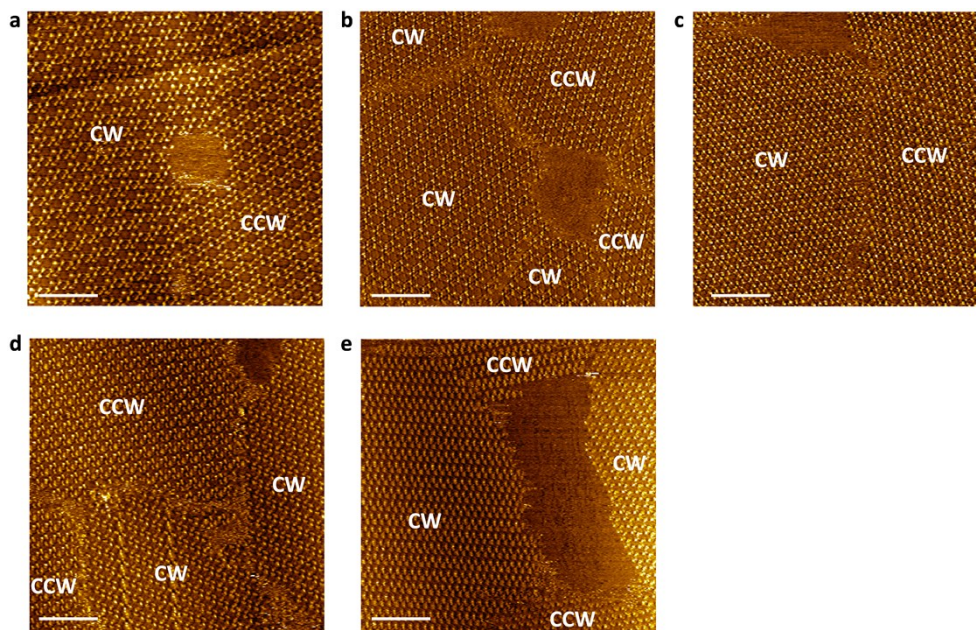


**Figure S2.** STM images of the surface monolayer of BIC derivatives at the racemic mixture of (*R*)-2-nonanol and (*S*)-2-nonanol/interface. (a) BIC-C10 trimer; (b) BIC-C8 trimer; (c) BIC-C6 trimer; (d) Co-assembled tetramer of BIC-C6 and BIC-C10; (e) BIC-C10 dimer. Scale bar: 16 nm. Average tunneling current ( $I_{set}$ ) = 0.5–1 nA and bias voltage ( $V_{bias}$ ) = 900 mV.

### 4. The energy gain when an co-adsorbed 1-octanol in CW domain is replaced by (*R*)-2-nonanol

**Table S1.** Simulated energies from MM simulations in multiple motifs co-assembled by BIC derivatives and alcohols.  $E_{CW}$ : the adsorption energies per alcohol of CW polymorphs preferred by (*R*)-2-nonanol. Energies are presented in kcal·mol<sup>-1</sup>.

	Trimer (BIC-C6)	Trimer (BIC-C8)	Trimer (BIC-C10)	Tetramer (BIC-C6 and BIC-C10)	Dimer (BIC-C10)
$E_{CW}$ (assembled by 1-octanol)	75.7	83.4	88.2	139.3	56.1
$E_{CW}$ (assembled by ( <i>R</i> )-2-nonanol)	78.1	85.6	89.6	140.0	58.1

## 5. MM simulations using Dreiding force field

In addition to MMFF force field, we have conducted the simulations using Dreiding force field. The results are shown in Table S2 below.

**Table S2.** Simulated energies from MM simulations in multiple motifs co-assembled by BIC derivatives and (*R*)-2-nonanol. Simulations were carried out using Dreiding force field. Energies per unit area are presented in kcal·mol<sup>-1</sup>·nm<sup>-2</sup>.

	Trimer (BIC-C6)	Trimer (BIC-C8)	Trimer (BIC-C10)	Tetramer (BIC-C6 and BIC-C10)	Dimer (BIC-C10)
$E_{CW}^a$	13.29	12.06	10.73	11.09	15.97
$\Delta E_{CW-CCW}^b$	1.40	1.03	0.51	0.31	0.11

<sup>a</sup> $E_{CW}$ : the total adsorption energies of CW polymorphs preferred by (*R*)-2-nonanol.

<sup>b</sup> $\Delta E_{CW-CCW}$ : the difference in adsorption energy between CW and CCW units constructed by BIC and (*R*)-2-nonanol.

**Table S3.** Contribution of hydrogen bonding or van der Waals interactions to the energy difference simulated using Dreiding force field. Energies per unit area are presented in kcal·mol<sup>-1</sup>·nm<sup>-2</sup>.

	Trimer (BIC-C6)	Trimer (BIC-C8)	Trimer (BIC-C10)	Tetramer (BIC-C6 and BIC-C10)	Dimer (BIC-C10)
Hydrogen bonding	1.283	0.924	0.509	0.392	0.254
van der Waals	0.151	0.021	0.003	-0.125	-0.098 <sup>a</sup>

<sup>a</sup> “-” means that the absolute value of van der Waals interactions in unfavorable conformation (Figure 3c in manuscript) is larger than that in favorable conformation (Figure 3b in manuscript). Directional hydrogen bonds are formed in favorable conformation at the expense of van der Waals interactions.

From the simulation results (Table S2) using Dreiding force field, we can find that the changed tendency of energy difference in different supramolecular assemblies is consistent with the calculations using MMFF force field. Moreover, the contributions of hydrogen bonding or van der Waals interactions to the energy difference shown in Table S3 indicate that hydrogen bonding make the major contribution to the energy difference.

## 6. Another unfavorable conformation

In order to confirm the unfavorable conformations, we have also conducted the simulation in which the hydroxy group of (*R*)-2-nonanol was rotated by 180 degrees to co-assemble into the CCW hydrogen bonding circles (Figure S3 below). Taking the BIC-C10 trimer as an example, in this case, in order to retain the stable hydrogen bonding circles, the relative positions of the BIC and co-adsorbed 2-nonanol are changed. The initial structure is supplied below (Figure S3 left). The alkyl chains in (*R*)-2-nonanol are no longer parallel to that in BIC. After optimization, the co-

adsorbed (*R*)-2-nonanol is adsorbed with methylene hydrogens orientated vertically, rather than typical flat-lying orientation, due to steric hindrance of stereogenic methyl group. Simulated adsorption energy per unit cell for this situation is  $-354.6 \text{ kcal}\cdot\text{mol}^{-1}$  while the energy value is  $-470.6 \text{ kcal}\cdot\text{mol}^{-1}$  for the unfavorable BIC-C10 trimer proposed in Figure 3c in the manuscript. Thus, the unfavorable adsorption conformation shown in Figure 3c in the manuscript is more energetically favored than the conformation in Figure S3 below and is chosen as the unfavorable arrangement.

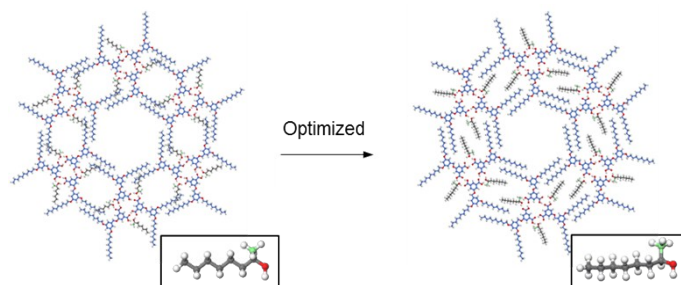


**Figure S3.** Interaction mode in which (*R*)-2-nonanol assembles into CCW motifs with the hydroxyl group rotated  $180^\circ$ . The co-assembled (*R*)-2-nonanol is colored gray for identification. The insets enlarge the co-adsorbed 2-octanol in corresponding conformation.

## REFERENCE

1. J. R. Gong, S. B. Lei, L. J. Wan, G. J. Deng, Q. H. Fan and C. L. Bai, *Chem. Mater.*, 2003, **15**, 3098-3104.
2. C. E. Kundrot, J. W. Ponder and F. M. Richards, *J. Comput. Chem.*, 1991, **12**, 402-409.
3. T. A. Halgren, *J. Comput. Chem.*, 1996, **17**, 490-519.
4. P. Ren, C. Wu and J. W. Ponder, *J. Chem. Theory Comput.*, 2011, **7**, 3143-3161.
5. C.-A. Palma, M. Bonini, A. Llanes-Pallas, T. Breiner, M. Prato, D. Bonifazi and P. Samori, *Chem. Commun.*, 2008, 5289-5291.